J. Fluid Mech. (1994), *vol.* 260, *pp.* 315–331

The stability of statically unstable layers

By S. A. THORPE

Department of Oceanography, The University, Southampton SO9 5NH, UK

(Received 23 February 1993 and in revised form 18 August 1993)

We investigate the development of instability in a fluid with density locally of the form $\rho_0[1-(N^2/g)z+A\sin Kz]$, composed of an overall stable uniform gradient of buoyancy frequency, N, but with a superimposed sinusoidal variation of vertical wavenumber, K, and amplitude, $A \ll 1$; g is the acceleration due to gravity and z is the upward vertical coordinate. Layers exist in which the fluid is statically unstable when the parameter $r = N^2/gKA$, is less than unity.

When r is zero, the density is sinusoidal in z and the problem reduces to one studied by Batchelor & Nitsche (1991). Their solution, which finds a gravest mode of linear instability with terms having vertical motions independent of z and with horizontal scales large in comparison with K^{-1}, is extended to non-zero r. An effect of a small, but finite, r is to stabilize the fluid, increasing the critical Rayleigh number and the corresponding non-dimensional horizontal wavenumber. The vertical scale of the mode which first becomes unstable is reduced as r increases. A small sinusoidal shear destabilizes the fluid.

When r approaches unity, the density field contains regions of static instability which are of thickness small compared to K^{-1}. The problem then approximates to one studied by Matthews (1988). Consistent solutions for the growth of disturbances are obtained by truncated series and, following Matthews, by the solution of a Fourier-transformed equation. A small uniform shear, characterized by a flow Reynolds number, $Re > 0$, is found to stabilize the fluid, in that it increases the critical Rayleigh number of the onset of instability. This suggests that convective Rayleigh–Taylor instability, with constant phase lines parallel to the flow, is then the favoured mode of onset of instability. At very large Rayleigh numbers and at a Prandtl number of 700, however, the growth rate of the most rapidly growing linear disturbances may increase as Re increases from zero, and the form of the evolving flow is then less certain.

The theory is used to estimate the scale and growth rates of instability in overturning internal gravity waves in the laboratory experiment described in a companion paper (Thorpe 1994).

1. Introduction

We consider the stability of a fluid having a vertical density profile given by

$$\rho_1 = \rho_0[1-(N^2/g)z+A\sin Kz], \tag{1}$$

where ρ_0 is a reference density, N is a real constant buoyancy frequency characterizing the overall stratification, g is the acceleration due to gravity, A ($\ll 1$) is a constant and K is a vertical, z-directed, wavenumber. This represents the density in a fluid which is in an overall state of stable stratification but, if $r = N^2/gKA < 1$, contains local layers of static instability as sketched in figure 1. These layers are of small vertical scale if r

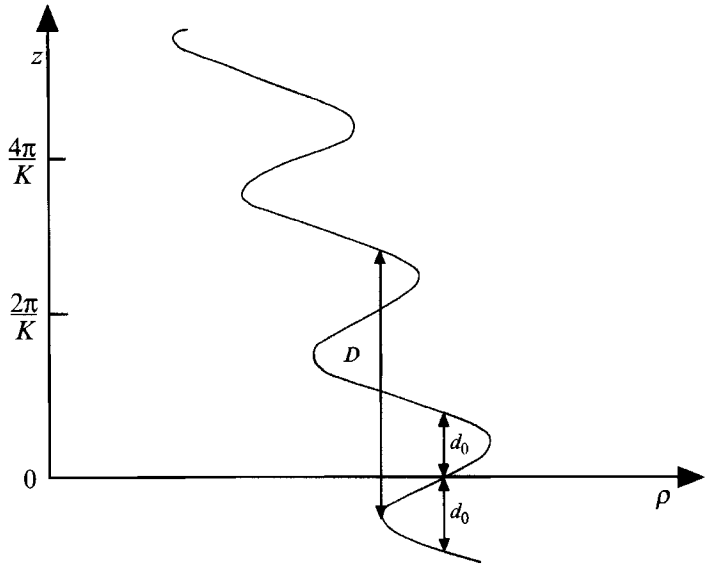

FIGURE 1. The form of the density profile (1) for $2/5\pi < r < 2/3\pi$. The overturn scale, d_0, and the maximum distance, D, of density exchange with conservation of density are shown. In this range of r there are as many as five levels, z, at which the same density can be found. (In general, $2n+1$ such levels occur when $2/[(2n+1)\pi] < r < 2/[(2n-1)\pi]$, $n = 1, 2, 3, \ldots$.) The vertical scale of convective overturn is found to be less than D.

is close to unity. Batchelor & Nitsche (1991, hereafter referred to as BN), examine the case $r = 0$ when there is no mean fluid flow, and find that a convective mode of instability of large horizontal and vertical scale is present, no matter how small is the characteristic Rayleigh number.

Patches of density microstructure in the ocean appear to have a vertical density distribution of the general form described by (1). It is, however, often the case that only a single vertical profile through a patch is obtained and nothing is known of the horizontal density structure or of the microscale velocity field. It is important to establish whether the presence of statically unstable regions in such profiles implies that the fluid is dynamically unstable (or perhaps even turbulent) or whether it may in fact be layered and stable. The study was, however, originally motivated by laboratory observations of breaking internal waves. The onset of conditions of 'breaking' is usually characterized by the overturn or folding of isopycnal surfaces so that, in some local region, the density decreases in the direction of gravity. Thin and horizontally extensive layers of statically unstable fluid can be produced in this way by large-amplitude internal waves in uniformly stratified fluids. We shall derive estimates for the growth rates and nature of instability in these layers which can be used to help explain the results of experiments and to predict the nature of instabilities which occur in the natural environment (Thorpe 1994).

We consider the stability of the fluid both when stationary and when in a state of horizontal flow with vertical shear which is maintained to be steady against the effects of viscosity. Steady flow is strictly possible only when the vertical gradient is uniform, so that (provided the kinematic viscosity is also uniform) the viscous terms associated with the mean flow in the Navier–Stokes equations vanish identically, or if the flow is maintained against viscosity by some external body force. Similar conditions are imposed regarding the diffusion of the nonlinear density profile (1). BN derive equations for the stability of stationary fluid containing statically unstable layers, and

point, in particular, to the inconsistency of choosing a nonlinear density profile which, in a diffusive fluid, will develop in time so that the basic density is unsteady, a factor ignored in the analysis. In the application to internal waves considered here, the flow and density fields are also developing, the latter as a consequence of fluid motions and diffusion. The governing equations applied to 'frozen' fields of motion and density, will serve, however, to establish growth rates for the instabilities which may be compared to the viscous and diffusive development of the density field and to the rates of change of the motion and flow modification of the density field, that is to the timescales of the internal waves. When the instability growth rates are sufficiently large, it may be appropriate to disregard the changing flow and the development of the density field in the overturned waves resulting either from diffusion or fluid motion.

We take a flow $(U(z), 0, 0)$ with a corresponding perturbation (u, v, w) and seek stationary solutions, arguing that these are contiguous to the zero flow solutions with which they are compared and, given the symmetrical nature of the velocity fields that we choose to select, there is no directional preference for disturbance propagation.

If the perturbation is independent of x and diffusion of the mean flow and density fields can be neglected, the linearized Boussinesq equations of motion reduce to a two-dimensional problem in the (y, z)-plane, and the stability equations reduces to

$$\left(\frac{\gamma}{\mathscr{D}}+\alpha^2-\frac{\mathrm{d}^2}{\mathrm{d}z^2}\right)\left(\frac{\gamma}{\nu}+\alpha^2-\frac{\mathrm{d}^2}{\mathrm{d}z^2}\right)\left(\alpha^2-\frac{\mathrm{d}^2}{\mathrm{d}z^2}\right)W=\frac{g\alpha^2}{\mathscr{D}\nu}\frac{1}{\rho_0}\frac{\mathrm{d}\rho_1}{\mathrm{d}z}W, \tag{2}$$

if the vertical velocity of the perturbation is written $w = W(z)\,e^{\gamma t}\cos\alpha y$, supposed periodic in y with wavenumber α, and with growth rate exponent γ, and $\mathscr{D}$ is the (constant) diffusivity of density and ν is the (constant) kinematic viscosity. This equation is identical to that derived by BN in the absence of mean flow, and is valid even when the mean flow is a function of time, as it is in the internal gravity waves. The solution, and the conditions at the onset of instability, are therefore identical to those found in the absence of shear. If, on the other hand, the perturbation is independent of y, the linearized Boussinesq equations may be combined into one equation for a stream function ψ, such that $u = \partial\psi/\partial z$ and $w = -\partial\psi/\partial x$, and

$$\left(\frac{\partial}{\partial t}+U\frac{\partial}{\partial x}-\mathscr{D}\nabla^2\right)\left[\left(\frac{\partial}{\partial t}+U\frac{\partial}{\partial x}-\nu\nabla^2\right)\psi-\frac{\mathrm{d}^2U}{\mathrm{d}z^2}\frac{\partial\psi}{\partial x}\right]+N_1^2\frac{\partial^2\psi}{\partial x^2}=0, \tag{3}$$

where $N_1^2 = -(g/\rho_0)\,\mathrm{d}\rho_1/\mathrm{d}z$ and $\nabla^2 = \partial^2/\partial x^2+\partial^2/\partial z^2$. When the disturbance is neutral with vanishing time derivatives, this equation can be written in the non-dimensional form

$$\nabla'^6\psi-Ra\,N_0^2\frac{\partial^2\psi}{\partial x'^2}=Re\frac{\partial}{\partial x'}\left\{(1+Pe)\,U'\nabla'^4\psi-Pr\,Re\,U'^2\frac{\partial}{\partial x'}\nabla'^2\psi+2\frac{\mathrm{d}U'}{\mathrm{d}z'}\frac{\partial}{\partial z'}\nabla'^2\psi\right.$$
$$\left.+Pr\,Re\,U'\frac{\mathrm{d}^2U'}{\mathrm{d}z'^2}\frac{\partial\psi}{\partial x'}-2\frac{\mathrm{d}^3U'}{\mathrm{d}z'^3}\frac{\partial\psi}{\partial z'}-\frac{\mathrm{d}^4U'}{\mathrm{d}z'^4}\psi\right\}. \tag{4}$$

Here $Pr = \nu/\mathscr{D}$, $Re = U_0 L/\nu$, $x' = x/L$, $z' = z/L$, where U_0 characterizes the velocity scale, $U' = U/U_0$, L is a characteristic lengthscale, and

$$Ra=\left.\frac{gL^4}{\nu\mathscr{D}\rho_0}\frac{\mathrm{d}\rho_1}{\mathrm{d}z}\right|_0 \tag{5}$$

with the density gradient, $\mathrm{d}\rho_1/\mathrm{d}z$, evaluated at some reference level $z = 0$ to characterize a positive (statically unstable) gradient, and N_0^2 is the negative square buoyancy frequency, non-dimensionalized with $\mathrm{d}\rho_1/\mathrm{d}z|_0$, so that for the chosen density (1),

$N_0^2 = \cos Kz - r$. If the critical Rayleigh numbers found as solutions of (2) are smaller that those of (3), a mode with y-directed wavenumber will grow before those with x-directed wavenumbers as the Rayleigh number is increased, and longitudinal rolls are more unstable than transverse billows (i.e. disturbances with constant phase lines directed normal to the flow).

The paper divides naturally into two parts. In the first we extend BN's results at $r = 0$ and examine small r (> 0), and a small specified mean shear. In the second we consider the stability at larger r (< 1), with particular attention to the case when r is just smaller than unity which characterizes the conditions as the isopycnal surfaces in internal waves first overturn.

2. Solutions for small values of r

2.1. *No shear*

The stability equation is then (2) which, on substituting for the ρ_1 from (1), becomes

$$\left(\frac{\gamma}{\mathscr{D}}+\alpha^2-\frac{\mathrm{d}^2}{\mathrm{d}z^2}\right)\left(\frac{\gamma}{\nu}+\alpha^2-\frac{\mathrm{d}^2}{\mathrm{d}z^2}\right)\left(\alpha^2-\frac{\mathrm{d}^2}{\mathrm{d}z^2}\right)W = \frac{\alpha^2 K^4\, Ra}{1-r}(\cos Kz - r)\, W, \tag{6}$$

where $Ra = gA(1-r)/(\mathscr{D}K^3)$ is a Rayleigh number, characterized by the maximum density gradient (at $z = 0$) and the lengthscale, K^{-1}, of the density profile. When $r = 0$, this equation and the Rayleigh number are identical to those used by BN. They write

$$W(z) = \sum_{n=1}^{\infty} F_n \sin nKz + \sum_{n=0}^{\infty} G_n \cos nKz, \tag{7}$$

substitute in (6), convert all terms to Fourier series, and hence find a set of linear equations relating the F_n and G_n by equating coefficients of odd and even Fourier components, $\sin nKz$ and $\cos nKz$, respectively. The odd and even components are not coupled and may be treated separately. Solutions are found by truncating the series (7) at some value $n = M_T$, terms with $n \geqslant M_T$ (later referred to as the truncation number) being set to zero. Terms F_n and G_n of increasingly large order, n, are found to have coefficients that are much larger than those of lower order, n, to which they are related in the set of linear equations, and therefore themselves decrease rapidly as n increases. Low-order truncation with $M_T = 2$ or 3 was found to give formulae relating the Rayleigh number and the wavenumbers, which provide quantitatively accurate approximations, with the advantage that these could be solved analytically. There exists a mode of instability which persists even when Ra approaches zero, so that the 'critical' Rayleigh number for the onset of instability is zero, and the density field is always unstable. This gravest mode of instability, the 'first even mode' in BN's classification, is characterized by non-vanishing vertical motion (i.e. G_0 is non-zero) with large horizontal scale. The physical mechanism leading to instability is one in which the denser layers slide towards disturbance wave troughs, while less dense layers move towards wave crests, thus leading to a horizontal variation in the vertically integrated density field which, via buoyancy forces, then reinforces the original perturbation.

For sufficiently small $r > 0$, we may anticipate that, as found by BN, low-order truncation will provide accurate prediction. The cosine terms in (6), with (7) substituted, are found to be

$$\sum_{n=0}^{\infty} G_n\left(L_n + \frac{r\alpha^2 K^4}{1-r}\right)\cos nKz = \frac{\alpha^2 K^4\, Ra}{2(1-r)} \sum_{n=0}^{\infty} G_n\{\cos[(n+1)\,Kz] + \cos[(n-1)\,Kz]\}, \tag{8}$$

where $L_n = (\gamma/\mathscr{D} + K^2n^2 + \alpha^2)(\gamma/\nu + K^2n^2 + \alpha^2)(K^2n^2 + \alpha^2)$. The appearance of terms of sixth-power in n as coefficients of G_n helps ensure rapid convergence of the series (7) and makes truncation with few terms a good approximation for low-order modes.

If we first truncate at $M_T = 2$, setting $G_n = 0$ for $n \geqslant 1$ and equating coefficients of $\cos nKz$ for $n = 0$ and 1, we find

$$G_0\left[L_0 + \frac{r\,Ra\,\alpha^2K^4}{1-r}\right] = \left[\frac{Ra\,\alpha^2K^4}{2(1-r)}\right]G_1, \tag{9}$$

and

$$G_1\left[L_1 + \frac{r\,Ra\,\alpha^2K^4}{1-r}\right] = \left[\frac{Ra\,\alpha^2K^4}{1-r}\right]G_0, \tag{10}$$

which, on eliminating G_0 and G_1, give a quadratic equation in Ra. The critical Rayleigh number for this mode is the minimum value of Ra that satisfies this condition as α/K is varied and when the neutral disturbance $\gamma = 0$ is selected.

When $r = 0$, elimination of G_0 and G_1 gives

$$Ra^2 = 2\alpha^2(\alpha^2 + K^2)^3/K^8, \tag{11}$$

and so Ra tends to zero as α/K tends to zero. This is the first even mode described by BN, with zero critical Rayleigh number and corresponding large horizontal wavenumber. The first, odd, and second, even, modes have critical Rayleigh numbers of 62.9 and 510 at $\alpha/K = 0.963$ and 1.70, respectively. Higher modes have larger critical Rayleigh numbers.

For non-zero r, (9) and (10) give an equation in Ra from which an approximate value of the critical Rayleigh number can be found when r is sufficiently small;

$$Ra_{crit} = 2r(1-r)/(1-2r^2) \quad \text{at} \quad \alpha/K = 2r. \tag{12}$$

The growth rates for Prandtl number $Pr = 1$ are given by

$$\Gamma = (\gamma/K^2\nu) = [Ra^2\,q/2 - Ra/(1-r)]^{\frac{1}{2}} - q, \tag{13}$$

where $q = (\alpha/K)^2 \ll 1$, and the maximum growth rates are

$$\Gamma = 2r(\phi^2 - \phi^{-1}) \tag{14}$$

at $q = 2r(1+\phi^3)/\phi$, where $\phi = 2\,Ra\,r/(1-r)$. Figure 2 shows both the approximate solution for the critical Rayleigh number and the corresponding α/K, together with the numerically determined solution of the quadratic equation. This has been verified as being accurate quantitatively by calculations with truncation at higher orders. The first odd and second even modes at $r > 0$ have larger critical Rayleigh numbers than at $r = 0$; for example, at $r = 0.1$, the first, odd, and second, even, modes have critical Rayleigh numbers of 87 and 610 at $\alpha/K = 1.1$ and 1.8, respectively.

The form of the series (7) chosen to seek solutions, however, is restrictive. As BN point out, Floquet theory indicates the existence of modes with period $2\pi M/K$, where M is an integer. Their first even mode, corresponding to $M = 1$, nevertheless remains the most unstable when $r = 0$. We have considered even-mode solutions of the form

$$W(z) = \sum_{n=0}^{\infty} G_{n,M}\cos(nKz/M). \tag{15}$$

Substitution into (6) with $\gamma = 0$ and comparing coefficients then results, as before, in a series of relations between coefficients. Truncation at $M_T = 2M+1$, so that

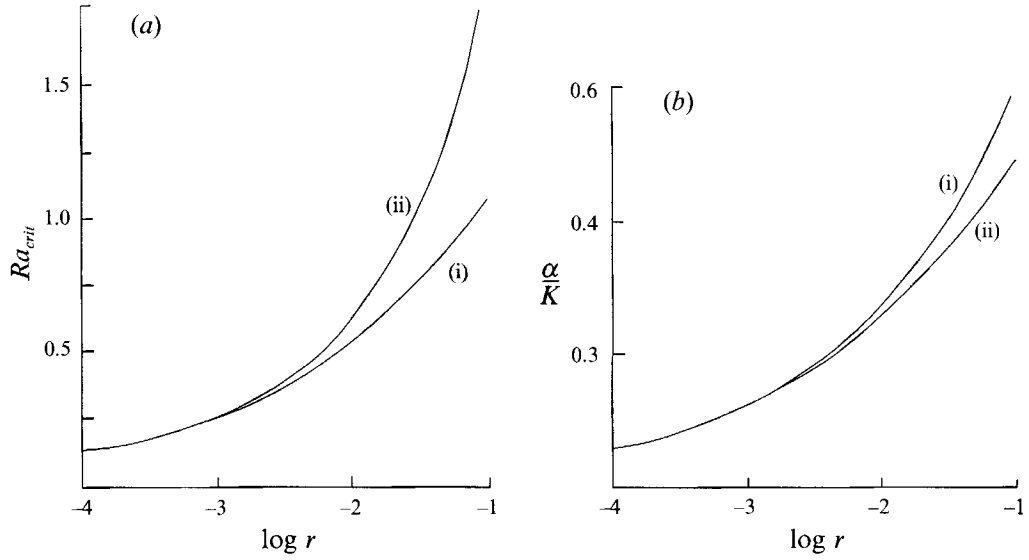

FIGURE 2. (*a*) The critical Rayleigh number, Ra_{crit}, for the first even mode as a function of r, showing the approximate small-r solution (i) and the exact solution to the governing quadratic equation (ii). (*b*) The corresponding non-dimensional wavenumber, α/K.

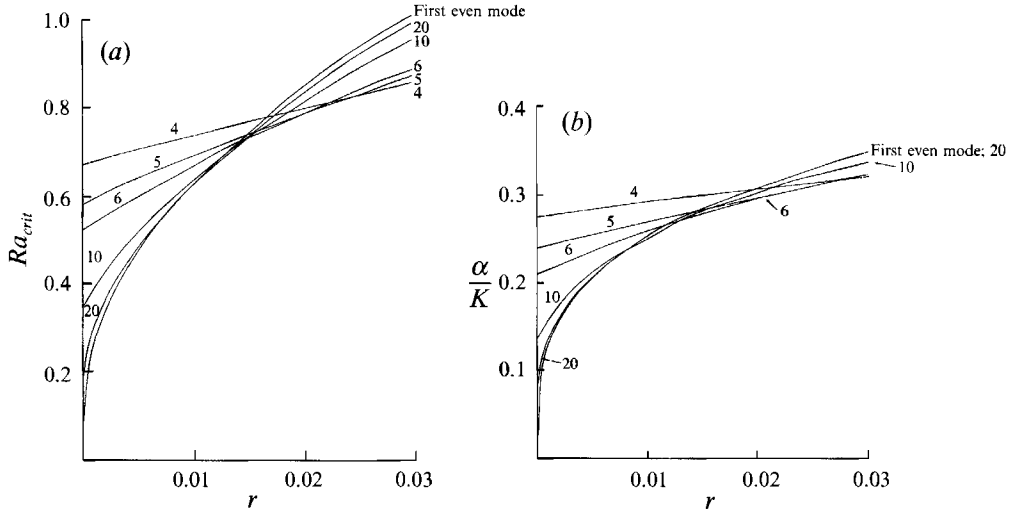

FIGURE 3. The critical Rayleigh number for the first even mode and the modes $M = 4$, 5, 6, 10 and 20 found by truncation at $M_T = 7$, as functions of r. (*b*) The corresponding non-dimensional wavenumbers, α/K.

$G_{n,M} = 0$, $n > 2M$, and elimination of the coefficients gives a set of equations, quartic in Ra, of the form

$$(L_{n,M+1}L_{n,1} - f^2)(L_{n,2M-1}L_{n,M-1} - f^2) = f^2 L_{n,2M-1}L_{n,M+1}, \tag{16}$$

where $L_{n,M} = (\alpha^2 + M^2K^2/N^2)^3 + 2rf$ and $f = \alpha^2 K^4\, Ra/[2(1-r)]$.

The solutions for the critical Rayleigh numbers and non-dimensional wavenumbers for $M = 4$, 5, 6, 10 and 20 are shown in figure 3. For $0 \leqslant r < 0.0102$, the first even-mode solution gives the smallest critical Rayleigh number in the set of modes

examined. For $0.0102 < r < 0.0113$, the mode with $M = 20$ corresponding to cellular convection on a vertical scale $40\pi K^{-1}$ gives the smallest critical Rayleigh number. The limit of stability transfers to $M = 10$, 6, 5 and to 4 at $r = 0.0113$, 0.0154, 0.0198 and 0.0248, respectively. The vertical scale of the mode is *less* than the scale of 'potential' overturn. For example, the mode $M = 5$ which marks the critical Rayleigh number in $0.0198 < r < 0.0248$ has a vertical scale of $10\pi K^{-1}$. In this range of r, the maximum vertical scale over which fluid particles may be exchanged without change in density, e.g. the scale D shown in figure 1, is given by $27\pi < DK < 33\pi$, and D is greater than $10\pi K^{-1}$. The sequential reduction in vertical scale as r increases is in accordance with the physically based expectation that the stabilizing effect of the stable linear component of the density (1) will eventually confine the vertical scale over which convection can develop. It also implies that solutions can be found in regions of z bounded by levels at which $w = 0$, which are such that ρ satisfies the physical conditions that it remain positive and finite. The analysis suggests that, for any value of $r > 0$, however small, there will be a mode at some value M (which increases as r decreases) which has a lower critical Rayleigh number than the first even mode. We shall consider again the transfer of stability between modes in §3.4.

2.2. *The effect of sinusoidal shear*

We consider for illustration a flow with $U = U_0 \sin Kz$. This choice is dictated by the perceived value of finding solutions towards which some progress can be made analytically, rather than by the need to match some particular flow field. We seek neutral solutions with vanishing time derivatives. In the present case, the existence of modes of oscillation at lower critical Rayleigh numbers than found earlier in a stationary fluid is a sufficient result for our purpose. In the absence of shear, $U_0 = 0$ and $Re = 0$ so that the terms on the right-hand side of (4) vanish, and the problem reduces to (6) with $\gamma = 0$.

We again seek a solution of the form (7). Recurrence relations (which are no longer separable) are found relating the F_n and G_n terms of the odd and even modes. These may be solved by truncation at some order M_T. Truncation at $M_T = 2$ leads to a cubic equation for Ra in terms of Re, Pr and non-dimensional wavenumber which, at small values of r and $Re^2(1+Pr)$, leads to a minimum Rayleigh number,

$$Ra_{crit} = 2r[1 - \tfrac{1}{6} Re^2(1+Pr)] \quad \text{at} \quad \alpha/K = 2r[1 + \tfrac{1}{12} Re^2(1+Pr)], \tag{17}$$

a solution that may be compared to (12); the shear reduces the critical Rayleigh number and increases the corresponding wavenumber.

Solutions at $M_T = 4$ have been computed and an example, at $r = 0.001$, is shown in figure 4. This confirms that the effect of small Re is to decrease the critical Rayleigh number and increase the wavenumber at which instability occurs, but demonstrates a sensitivity to truncation at large Re which deserves further study. Similar behaviour is found for $M_T = 4$ at $r = 0.004$. Recalling the comments following (5), these results imply that as the shear increases from zero, a perturbation that is independent of y will have a smaller critical Rayleigh number than one independent of x; a mode with constant phase lines transverse to the flow direction will grow more rapidly than longitudinal rolls. This effect is expected, given the known properties of sinusoidal velocity profiles in destabilizing stably or neutrally stratified inviscid and non-diffusive fluids (e.g. Thorpe 1969). The increase in horizontal wavenumber is perhaps counter to the expectation that the mean flow might augment the redistribution of density leading to the physical mechanism of instability at large scale described in BN, and hence increase the dominant wavelength. The solution is a counter-example to the hypothesis

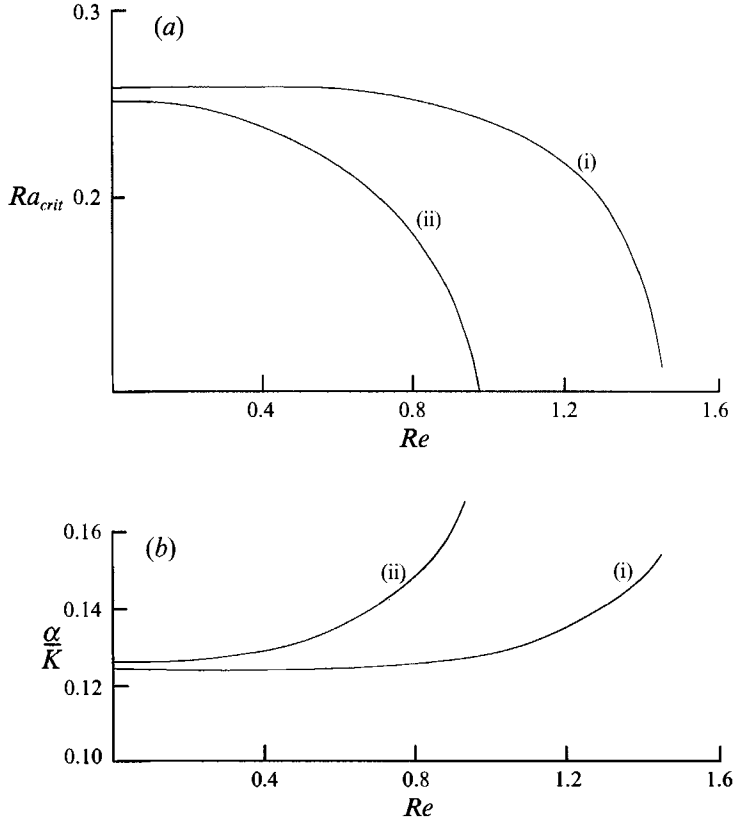

FIGURE 4. (*a*) The variation of critical Rayleigh number and (*b*) the corresponding non-dimensional wavenumbers, α/K, with Re at $r = 0.001$ for a sinusoidal shear flow. Curves (i) show the solution with $M_T = 4$, and (ii) the approximate solution given by (17).

that the effect of small shear will always promote instability with fastest growing wavenumber directed across the flow direction, although this is often found (e.g. Winters & Riley 1992).

3. Stability at finite $r < 1$

3.1. *Matthews' results*

Matthews (1988) considers the stability of a stationary fluid with density given by

$$\rho_1 = \rho_0(1 + B_1 z - A_1 z^3), \tag{18}$$

resembling a region of static instability embedded in a stable density gradient, and we shall show how his results may be used to provide approximate solutions. He defines a Rayleigh number, $Ra_M = gB_1 d^4/\nu\mathscr{D}$, using the scale $d = (B_1/A_1)^{\frac{1}{2}}$, the height, z at which the density is equal to the density at $z = 0$, and the measure, B_1, of the density gradient at $z = 0$. In an unbounded fluid, solutions are found by taking the Fourier transform of the stability equation (10) with $\gamma = 0$, giving an equation for

$$\hat{W}(q) = \int_{-\infty}^{\infty} \exp(-\mathrm{i}qz)\, W(z)\, \mathrm{d}z. \tag{19}$$

The boundary conditions are $\hat{W}(0) = 1$ and $\mathrm{d}\hat{W}/\mathrm{d}q = 0$ at $q = 0$, in the expectation of an even-valued lowest eigenvalue. The transformed equation is integrated numerically from $q = 0$ using a Runge–Kutta shooting method, the Rayleigh number being varied for each selected wavenumber until $\hat{W}$ approaches zero at large values of q. The critical Rayleigh is found to be 88.0 at a non-dimensional wavenumber $\alpha d = 1.26$. The instability takes the form of a cell extending to $z = \pm 1.69d$, with small counter-rotating cells above and below. When stress-free boundaries are introduced at $z = \pm L$, a solution is found by writing W as a cosine series

$$W(z) = \sum_{n=1}^{\infty} G_n \cos[(n-\tfrac{1}{2})\pi z/L], \tag{20}$$

substituting into the stability equation (2) with $\gamma = 0$, multiplying by $\cos[(m-\frac{1}{2})\pi z/L]$ and integrating from $z = -L$ to L to give a recurrence relation between the G_n. Solution is found by truncation at some order M_T. When L/d is greater than about 2.5, the critical Rayleigh number and corresponding wavenumbers are close to those in the absence of boundaries. As L/d decreases, the presence of the boundaries affects the structure of the unstable mode and first increases, then decreases, and finally again increases the critical Rayleigh number. A weakly nonlinear analysis is used to show that the bifurcation at the critical Rayleigh number is supercritical and that roll disturbances are preferred to squares for all values of the Prandtl number.

For small values of Kz, the density given by the model equation (1) approximates to

$$\begin{aligned}\rho_1 &= \rho_0[1-(N^2/g)\,z + A\{Kz - \tfrac{1}{6}(Kz)^3 + \ldots\}] \\ &= \rho_0[1 + A\{(1-r)\,Kz - \tfrac{1}{6}(Kz)^3 + \ldots\}],\end{aligned} \tag{21}$$

since $r = N^2/gKA$, so (1) approximates to (18) if

$$B_1 = A(1-r)\,K \quad \text{and} \quad A_1 = \tfrac{1}{6}AK^3. \tag{22}$$

Assuming that, when r is sufficiently close to unity, instability is determined by the density structure in and near the region of static instability close to $z = 0$ (and separately in the other regions of static instability near $z = 2n\pi K^{-1}$, $n = \pm 1, \pm 2, \ldots$ of (1)), the similarity of the density profiles implies that we may therefore use Matthews' results to predict the onset of instability near $r = 1$ in a fluid with density (1).

The relationship between the Rayleigh number $Ra = gA(1-r)/\mathscr{D}K^3$, and that used by Matthews, Ra_M, is $Ra = Ra_M/(36(1-r)^2)$, and we may therefore anticipate (recalling Matthews' finding that the critical $Ra_M = 88.0$ at $\alpha d = 1.26$) that, near $r = 1$, the critical Rayleigh number is

$$Ra = 88.0/(36(1-r)^2) = 2.44/(1-r)^2, \tag{23}$$

at the non-dimensional wavenumber $\alpha/K = 1.26(6(1-r))^{\frac{1}{2}}$ since $dK = (6(1-r))^{\frac{1}{2}}$. Given Matthews' results relating to the effect of boundaries, we may also anticipate that when the semi-period of the density, πK^{-1} exceeds a value of about $2.5d$, that is when $dK = (6(1-r))^{\frac{1}{2}} < \pi/2.5$, or $r > 0.75$, the development of instability in one statically unstable layer (say that surrounding $z = 0$) will be unaffected by that at neighbouring levels surrounding $z = \pm 2\pi K^{-1}$.

When r is not close to unity, we may 'fit' the density profiles (1) and (18) by equating the density gradients at $z = 0$, and by matching the vertical structure by equating the height d of (18) to the vertical scale of the smallest non-zero z, d_0, at which the density in (1) is equal to that at $z = 0$ (see figure 1). The value of d_0 is given by the smallest non-zero solution of

$$\sin Kd_0 = rKd_0. \tag{24}$$

We now proceed as follows. We use Matthews' Fourier transform method to extend his results in an infinite fluid with density (18) and to estimate the growth rates of unstable disturbances (§3.2). This will allow us to infer the growth rates of disturbances to (1) at sufficiently large r, < 1. We then, in §3.3, seek solutions of the form (20) which satisfy (6) and the condition $W = 0$ at $z = \pm\pi K^{-1}, = \pm L$, at the stably stratified interface between neighbouring regions of static instability, in the expectation that this will be the appropriate form of solution when r is large and < 1. In both cases we shall seek the maximum growth rates and corresponding non-dimensional wavenumbers at fixed values of the Rayleigh number. We then, in §3.4, relax the condition that the vertical motion is forced to be zero at $z = \pm L$, seeking solutions instead with boundaries at $z = \pm ML$, where M is an integer > 1. These solutions are found to have lower critical Rayleigh numbers only at values of r significantly less than unity, supporting the conjecture that solutions with structure that remains local to the regions of static instability at $z = 2M\pi K^{-1}$ dominate the onset of instability at large $r < 1$. Finally, in §3.5, we consider the effect of a mean uniform shear.

3.2. *The growth rates for Matthews' density profiles; no shear*

Equation (2), with ρ_1 given by (18) and lengths scaled with $d = (B_1/A_1)^{\frac{1}{2}}$, becomes

$$\left(Pr^{\frac{1}{2}}s+\beta^2-\frac{\mathrm{d}^2}{\mathrm{d}z^2}\right)\left(P_r^{-\frac{1}{2}}s+\beta^2-\frac{\mathrm{d}^2}{\mathrm{d}z^2}\right)\left(\beta^2-\frac{\mathrm{d}^2}{\mathrm{d}z^2}\right)W = Ra_M\beta(1-3z^2)\,W, \tag{25}$$

where $\beta = \alpha d$ is the non-dimensional wavenumber, and z is now the vertical coordinate scaled with d and $s = d^2\gamma/(\nu\mathscr{D})^{\frac{1}{2}}$ is the non-dimensional growth rate, The equation for the Fourier transform, $\hat{W}(q)$, is then

$$3\,Ra_M\beta^2\,\mathrm{d}\hat{W}/\mathrm{d}q^2 = [(Pr^{\frac{1}{2}}s+\beta^2+q^2)(Pr^{-\frac{1}{2}}s+\beta^2+q^2)(\beta^2+q^2)-Ra_M\beta^2]\,\hat{W}, \tag{26}$$

with $\mathrm{d}\hat{W}/\mathrm{d}q = 0$ at $q = 0$. $\hat{W}(q)$ tends to zero as q tends to infinity, and $\hat{W}(0)$ is normalized to unity. We follow Matthews' (1988) method of solution, seeking the minimum Rayleigh number, $\min Ra_M$, for each specified value of s, and the corresponding β, β_m. For $s = 0$, this gives the critical Rayleigh number, whilst the variation of $\min Ra_M$ with β_m gives the locus of Rayleigh numbers and wavenumbers that have the maximum growth rates as Ra_M increases.

Solutions for $Pr = 1$ and 700 are shown in figure 5. They converge to Matthews' critical Rayleigh number at $s = 0$. The non-dimensional wavenumbers, β_m, increase, indicating that, at $Ra_M > \min Ra_M$, the horizontal wavenumber of the fastest growing waves will be less than that at which instability first occurs as Ra_M increases through $\min Ra_M$.

3.3. *The growth rates. Vertically bounded solutions; no shear*

Non-dimensionalizing (6) using the scale K^{-1} gives

$$\left(Pr^{\frac{1}{2}}\Gamma+q^2-\frac{\mathrm{d}^2}{\mathrm{d}z^2}\right)\left(Pr^{-\frac{1}{2}}\Gamma+q^2-\frac{\mathrm{d}^2}{\mathrm{d}z^2}\right)\left(q^2-\frac{\mathrm{d}^2}{\mathrm{d}z^2}\right)W = \frac{Ra\,q^2}{1-r}(\cos z-r)\,W, \tag{27}$$

where z is written for Kz, $q = \alpha/K$ and $\Gamma = \gamma(K^2(\nu\mathscr{D})^{\frac{1}{2}})$ is the non-dimensional growth rate. The Rayleigh number is that defined below (6). Comparison of coefficients of successive cosine terms when (20) is substituted into (27) results in a set of equations, each forming a relation between 2 or 3 of the coefficients G_n, which may be solved when the series (20) is truncated at some value, M_T, chosen here as 7 or 9. As r increases towards unity, the vertical scale of the statically unstable region diminishes and in

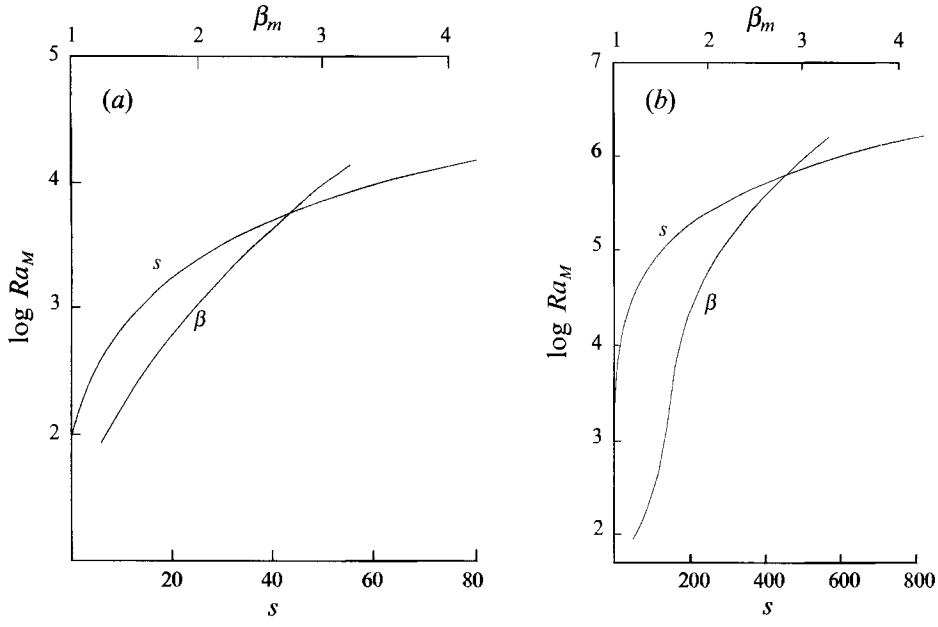

FIGURE 5. The maximum growth rates, s, and corresponding wavenumbers, β_m, for the cubic density profile (18) as functions of Ra_M at (*a*) $Pr = 1$, and (*b*) $Pr = 700$.

order to resolve the unstable convective motion in this region, the number of terms in the series must increase correspondingly. It is therefore impractical to use this form of solution very close to $r = 1$, but here the correspondence with Matthews' solution may be used to find solutions.

We have, as in §3.2, chosen to specify the growth rate and to seek the smallest Rayleigh number at which this rate can be attained. In order to relate the growth rates to the characteristics of the physical environment within which the regions of static instability are embedded, we have chosen to display the rates as the non-dimensional rate $\gamma_1 = \gamma/N$, where N is the buoyancy frequency of the background stable stratification in (1); $\gamma_1 = \Gamma((1-r)/Rar)^{\frac{1}{2}}$. For comparison with the results of §3.2, we use the maximum density gradient (at $z = 0$) and the vertical scale d_0 of the density profile to define a new Rayleigh number, R, scaled with d_0 rather than K^{-1}, and non-dimensional wavenumber, $m_0 = \alpha d_0$. The conversion relations are $R = (Kd_0)^4\, Ra$, where Kd_0 is found as the solution of (24), $R = Ra_M(d_0/d)^4$, $\gamma_1 = s((1-r)/rR)^{\frac{1}{2}}$, $\alpha d_0 = q(Kd_0)$ and $\alpha d_0 = \beta(d_0/d)$.

Examples of the results are shown in figure 6 at $Pr = 1, 7$ (typical of thermally stratified oceanic waters) and 700 (typical of the salt-stratified laboratory experiments). As expected, there is generally good agreement between the values found by the two different methods at the larger values of r, confirming our hypothesis that the use of Matthews' results to describe the onset, structure and development of instability for r near unity will provide accurate predictions. At $r = 0.5$, however, the vertically bounded truncated series gives systematically lower growth rates and wavenumbers than the unbounded Fourier transform solution, except at values of $R < 300$, where the unbounded solution has lower growth rates. Figure 6 shows how, at $Pr = 7$, the maximum growth rates increase with r at constant values of R. The maximum growth rates at fixed values of R and r decrease with increasing Pr. For example, at $R = 10^4$, $r = 0.8$, we find $\gamma_1 = 0.31$, 0.28 and 0.10 at $Pr = 1$, 7 and 700, respectively.

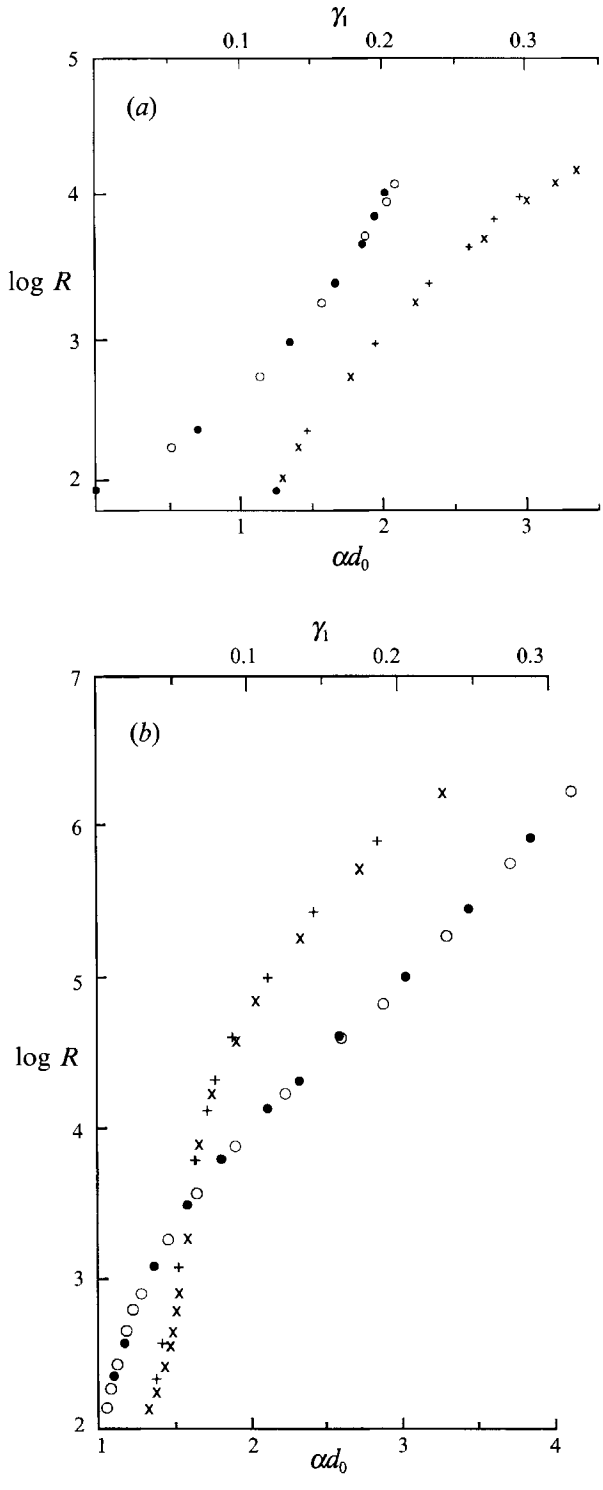

FIGURE 6(*a*, *b*). For caption see facing page.

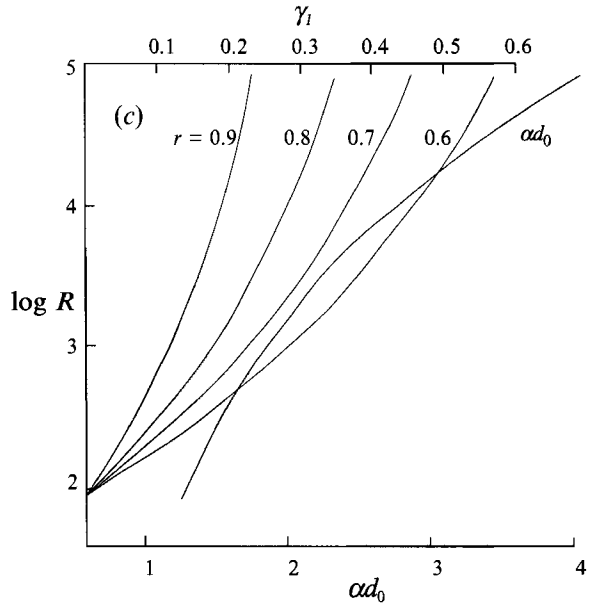

FIGURE 6. The variation of the maximum non-dimensional growth rate, $\gamma_1 = \gamma/N$, Rayleigh number, R, and corresponding wavenumbers, αd_0, at (*a*) $Pr = 1$, $r = 0.9$; (*b*) $Pr = 700$, $r = 0.8$. In each case solid and open circles show γ_1 values for the truncated series solution (§3.3) and Fourier transform solutions (§3.2) respectively. Plus signs and crosses show αd_0 values for the truncated series and Fourier solutions respectively. (*c*) The variation of γ_1 and αd_0 with R at $Pr = 7$ calculated from the Fourier transform solution. Values of γ_1 are given for $r = 0.6$ to 0.9.

The critical Rayleigh number, calculated using the bounded truncated series, shows a behaviour with r similar to that of the variation of Ra_M with L/d found by Matthews (figure 7). The Rayleigh number is sensibly constant with a value near 88 for $r > 0.7$ (large L/d), then rises to a maximum near $r = 0.6$ before falling to a minimum near $r = 0.3$, and then increasing once again, as r decreases and the scale height d_0 increases. This curve was calculated with truncation number $M_T = 9$ for $r \geqslant 0.5$, and $M_T = 7$ for $r < 0.5$. Values of R are, however, accurately predicted for $r < 0.6$ with $M_T = 3$ and for $r < 0.8$ with $M_T = 4$.

An example of the vertical structure of the unstable mode at $Pr = 1$, $r = 0.95$ at $\gamma_1 = 0.123$ calculated with truncation at $M_T = 9$, is shown in figure 8. As in Matthews' example, the vertical extent of the cellular motion around $z = 0$, the height to the first point at which $W = 0$, exceeds the scale d_0, and there are weak counter-rotating motions above and below.

3.4. *Instability at larger vertical scale and at moderate values of r; no shear*

We have sought solutions to (6), with $\gamma = 0$, of the even-mode form

$$W(z) = \sum_{n=0}^{\infty} G_{n,M} \cos[(2n+1)Kz/2M], \tag{28}$$

which satisfy a boundary condition $W = 0$ at $z = \pm M\pi K^{-1}$ (the case $M = 1$ corresponds to the solution described in §3.3), and of the odd mode

$$W(z) = \sum_{n=0}^{\infty} F_{n,M} \sin[(2n+1)Kz/2M], \tag{29}$$

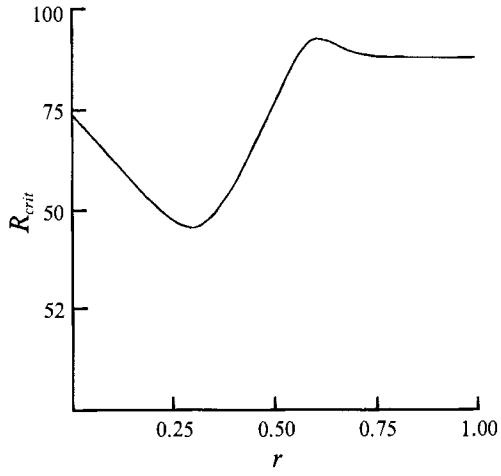

FIGURE 7. The variation of the critical Rayleigh number, R, with r.

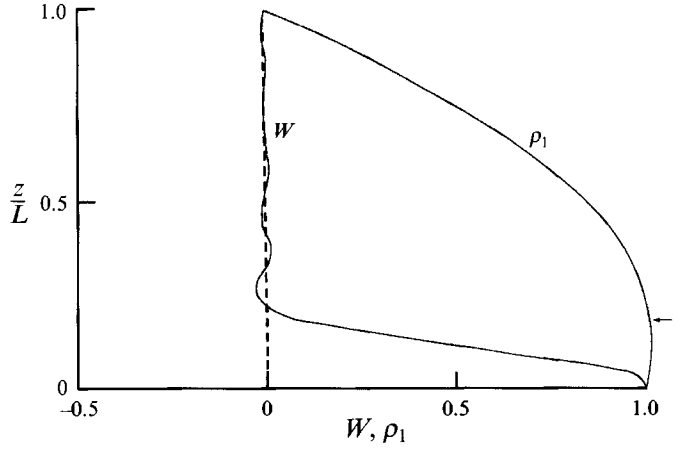

FIGURE 8. The solution for the vertical velocity, W, of the most unstable mode at $Ra = 49300$ and $Pr = 1, \alpha/K = 4.4$, together with the corresponding density variation, ρ_1. The arrow shows the height, d_0, at which the density is equal to that at $z = 0$. The convecting cell, centred at $z = 0$, extends to the level at which W is first zero, at a height exceeding d_0.

satisfying $W = 0$ at $z = 0$ and $z = \pm 2M\pi K^{-1}$, in the expectation that, at sufficiently small r, modes will be excited in which convective cellular motions extend vertically to involve two or more statically unstable regions, as found earlier in §2.1. Solutions are found by series truncation and comparison of coefficients.

The minimum Rayleigh numbers, Ra, and corresponding horizontal non-dimensional wavenumbers α/K, are shown in figure 9, using truncation at $M_T = 7$. Exchange of the onset mode of instability from the even mode $M = 1$ to the odd mode $M = 2$ does not occur until r falls to 0.033, much less than the value $r = 2/3\pi$ at which the density in one unstably stratified layer (e.g. that around $z = 0$ in figure 1) may be equal to that in another neighbouring layer (e.g. that around $z = 2\pi K^{-1}$). The subsequent transfer to the even mode $M = 3$ occur at $r = 0.024$. The modes have smaller critical Rayleigh numbers than the BN first even mode at sufficiently large r, as expected from the results presented in §2.1. Comparison of the solutions with

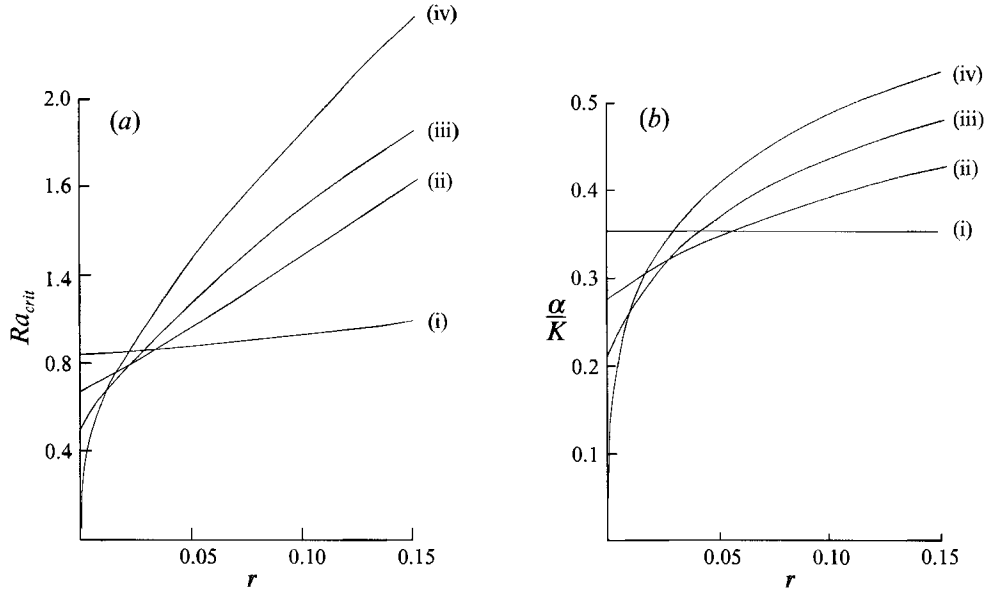

FIGURE 9. The variation of (*a*) the critical Rayleigh number, and (*b*) the corresponding non-dimensional wavenumber, α/K, with r for (i) the even mode with $M = 1$, (ii) the odd mode with $M = 2$; and (iii) the even mode with $M = 3$. Also shown is (iv) the solution corresponding to BN's first even mode. Truncation is at $M_T = 7$.

$M = 1, 2, 3$ at intermediate values of r (0.4, 0.5) shows that the even mode $M = 1$ continues to have the lowest Rayleigh number.

3.5. *The effect of a uniform mean shear*

For comparison with §2.2 (and having in view the application to internal waves; Thorpe 1994), we consider the effect of a mean shear, $U = U'z$, on the localized instability when r is less than, but close to, unity. Here U' is the constant shear, and without loss of generality, we have taken U to be zero at $z = 0$. Since we seek a solution near $r = 1$, it is appropriate to use the locally approximate density distribution (18).

Equation (8) simplifies to

$$\left[\left(\beta^2-\frac{\mathrm{d}^2}{\mathrm{d}z^2}\right)^3-Ra_M\beta^2(1-3z^2)\right]W$$

$$=\mathrm{i}\beta Re\left[2\frac{\mathrm{d}}{\mathrm{d}z}-z(1+Pr)\left(\beta^2-\frac{\mathrm{d}^2}{\mathrm{d}z^2}\right)+\mathrm{i}\beta z^2\,Pr\,Re\right]\left(\beta^2-\frac{\mathrm{d}^2}{\mathrm{d}z^2}\right)W, \quad (30)$$

where $Re = U'd^2/\nu$, the equation is non-dimensionalized as in §3.2, and we seek a solution proportional to $\exp(\mathrm{i}\beta x)$. The Fourier transform then gives

$$\beta^2[3\,Ra_M-Re^2\,Pr\,(\beta^2+q^2)]\frac{\mathrm{d}^2\hat{W}}{\mathrm{d}q^2}=\beta\,Re\,[4q\beta\,Re\,Pr+(1+Pr)\,(\beta^2+q^2)^2]\frac{\mathrm{d}\hat{W}}{\mathrm{d}q}$$

$$+\{(\beta^2+q^2)^3-Ra\,\beta^2+2\,Re\,\beta[\beta\,Re\,Pr+q(\beta^2+q^2)\,(2\,Pr+3)]\}\,\hat{W}, \quad (31)$$

which can be solved as in §3.2 by Runge–Kutta shooting.

At $Pr = 1$, the critical Rayleigh number is found to increase approximately linearly with Re from its value of 88 at $Re = 0$, to 200 at $Re = 2.7$. The critical wavenumber, β,

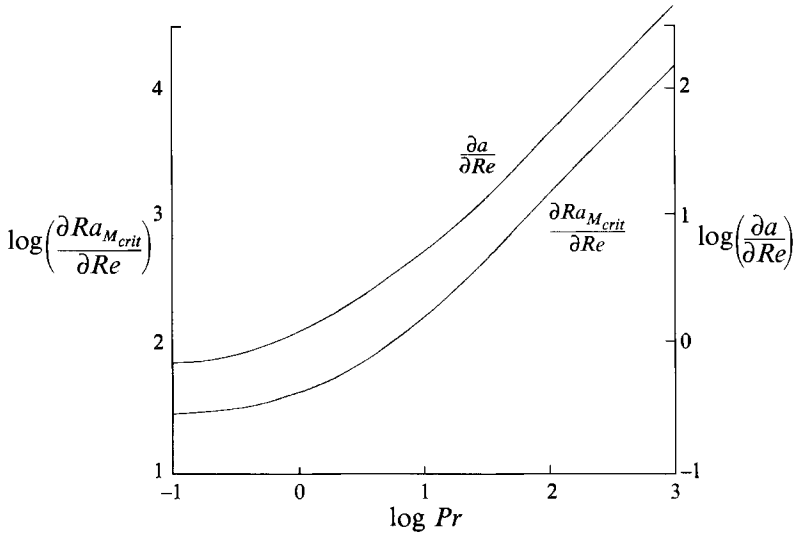

FIGURE 10. The variation with Pr of the derivative with respect to the Reynolds number, Re, of the critical Rayleigh number, Ra_{crit}, and the corresponding horizontal wavenumbers, α, evaluated at $Re = 0$, for a uniform shear flow and cubic density (18).

also increases, reaching 1.56 at the same Reynolds number. Figure 10 shows the derivative of the critical Rayleigh number with respect to the Reynolds number at constant Pr, evaluated at $Re = 0$, as a function of Pr, and the derivative with respect to Re of the wavenumber at which the critical Rayleigh number is found. Both derivatives are positive throughout the range of Prandtl numbers considered, with increasing values as Pr increases. Longitudinal rolls in the streamwise direction are therefore the preferred mode of the onset of instability, supposing it to be determined by the linear equations. This contrasts to the findings in §2.2.

We have examined the fastest growing disturbances at $Pr = 700$ at some selected values of Ra_M to provide estimates that relate to the experiments described by Thorpe (1994). At $Ra_M = 15000$, these are found at $Re = 0$, the most rapidly growing having $\beta = 1.8$ and growth rate $s = 28.9$. An increase of Re to 0.5 for $1 < \beta < 3$ reduces the growth rate of all waves; the fastest growing have $\beta = 2.0$ and $s = 21.2$. Similar behaviour is found at $Ra_M = 500000$, a Reynolds number increase from 0 to 1 reducing the fastest growth rate from 384.6 to 384.2, and increasing the associated wavenumber, β, from 2.75 to 2.85. At $Ra_M = 1.51 \times 10^6$, however, the fastest growing mode at $Re = 0$ has $s = 762.7$ at $\beta = 3.25$, but *larger* growth rates are found as Re increases up to a value of 6 (the largest value for which numerical convergence could be obtained), with

$$s = 762.7 + 3.37\,Re - 0.188\,Re^2 \tag{32}$$

and $\beta = (3.26 + 0.08\,Re) \pm 0.1$ providing good fits to the maximum growth rates and corresponding wavenumbers.

4. Discussion

In §2.1 we showed that the effects of global instability described by BN, with very large horizontal and vertical scales and with critical Rayleigh number of zero, are modified by a small, stable stratification, $0 < r \ll 1$. As illustrated in figure 2, the effect

of increasing r from zero is to increase the critical Rayleigh number and to reduce both the horizontal and vertical scales of the disturbance modes that first become unstable. The same effect was demonstrated in §3.4 where it was shown how, as the overall stratification and $r(<1)$ were reduced, the vertically limited mode of convection described by Matthews (1988) is modified, modes with lower critical Rayleigh numbers and larger vertical scales becoming dominant and characterizing the onset of instability at sufficiently low values of r. For $r < 2/3\pi$, the density distribution is such that at every level, z, there is fluid either of greater density above or of smaller density below. In this sense, the whole fluid column is unstably stratified. Nevertheless, the infinite fluid appears to be *stable* to infinitesimal disturbances provided the Rayleigh number is sufficiently small. Care may be needed, therefore, to properly interpret the state of motion inferred to occur in a fluid on the basis of single vertical profiles of density through patches of density microstructure in the ocean. A small sinusoidal shear reduces the critical Rayleigh number at $Pr = 1$ (§2.2).

The results of §3 are tested in an examination of the stability and evolution of overturning internal waves in a companion paper (Thorpe 1994). We should, however, recall here that the size of disturbances, at some time after conditions occur in which their growth is first possible, will depend on a time integration of the growth rates. These are determined by the temporal changes in the parameters, as well as the amplitude of the initial disturbances; the disturbances which, in practice, first become detectable may be different from those which first become unstable. In practice nonlinear effects may be important, particularly at the highly supercritical Rayleigh numbers considered in §3. The estimates of growth rates therefore provide at best a guide to the possible behaviour of disturbances that occur. In the conditions described in §3 when r is close to, but less than, unity, we have shown that the longitudinal disturbances have the smallest critical Rayleigh number when the Reynolds number is greater than zero, but small. These are expected to dominate at an early stage of growth. Moreover, for moderately supercritical values of the Reynolds number longitudinal disturbances have greater growth rates than transverses disturbance. There is, however, uncertainty about the fastest growing disturbances at highly supercritical values of the Rayleigh number and small Reynolds numbers, in particular when the Prandtl number, $Pr = 700$. Study of the finite-amplitude development of instability would be of value and might most profitably be made by numerical techniques.

The analysis described above was made at the Centre for Water Research at the University of Western Australia during a period of study leave in 1992. I am grateful to the CWR and the Royal Society for financial support which made the very pleasant visit possible.

REFERENCES

BATCHELOR, G. K. & NITSCHE, J. M. 1991 Instability of stationary unbounded stratified fluid. *J. Fluid Mech.* **227**, 357–391 (referred to herein as BN).

MATTHEWS, P. C. 1988 A model for the onset of penetrative convection. *J. Fluid Mech.* **188**, 571–583.

THORPE, S. A. 1969 Neutral eigensolutions of the stability equation for stratified shear flow. *J. Fluid Mech.* **36**, 673–683.

THORPE, S. A. 1994 Statically unstable layers produced by overturning internal gravity waves. *J. Fluid Mech.* **260**, 333–350.

WINTERS, K. B. & RILEY, J. J. 1992 Instability of internal waves near a critical level. *Dyn. Atmos. Oceans* **16**, 249–278.